LAWRENCE
LIVERMORE
NATIONAL
LABORATORY

UCRL-PROC-204120

Shock Initiation of Heterogeneous Explosives

John E. Reaugh

May 12, 2004

International Conference New Models and Hydrocodes for Shock Wave Processes
College Park, MD, United States
May 16, 2004 through May 20, 2004

Shock Initiation of Heterogeneous Explosives

John E. Reaugh
Physics and Applied Technologies Directorate
and
Energetic Materials Center
Lawrence Livermore National Laboratory
Livermore, CA 94551 USA

Abstract

The fundamental picture that shock initiation in heterogeneous explosives is caused by the linking of hot spots formed at inhomogeneities was put forward by several researchers[1,2] in the 1950's and 1960's, and more recently[3-5]. Our work uses the computer hardware and software developed in the Advanced Simulation and Computing (ASC) program of the U.S. Department of Energy to explicitly include heterogeneities at the scale of the explosive grains and to calculate the consequences of realistic although approximate models of explosive behavior. Our simulations are performed with ALE-3D, a three-dimensional, elastic-plastic-hydrodynamic Arbitrary Lagrange-Euler finite-difference program, which includes chemical kinetics and heat transfer, and which is under development at this laboratory.

We developed the parameter values for a reactive-flow model to describe the non-ideal detonation behavior of an HMX-based explosive from the results of grain-scale simulations. In doing so, we reduced the number of free parameters that are inferred from comparison with experiment to a single one – the characteristic defect dimension. We also performed simulations of the run to detonation in small volumes of explosive. These simulations illustrate the development of the reaction zone and the acceleration of the shock front as the flame fronts start from hot spots, grow, and interact behind the shock front. In

this way, our grain-scale simulations can also connect to continuum experiments directly.

Reactive flow model

The fundamental reactive flow model[6] is a rate law that describes the chemical change from the reactant, which is the unreacted solid explosive, to product, which is a mixture of gases with, perhaps, some solid particulates such as graphite, diamond, and metal oxide. The rate law incorporates separate terms for ignition and growth to completion of the reaction. In some versions of the model, the ignition term is consistent with the idea of a shock wave collapsing gas-filled cavities (defects) and creating a localized hot spot. In other versions, it is consistent with the idea of localized shear bands creating hot surfaces. The growth to completion of reaction is consistent with the idea of a subsonic deflagration of the explosive moving from each hot spot outward. The surface area at the flame front increases as the deflagration proceeds outward from a localized hot spot. Eventually the flame fronts arising from multiple hot spots intersect, and the available surface area at the overall flame front decreases as the reaction completes. The changing surface area, which relates the mass rate of burning to the flame velocity, is represented by a form factor that depends on the extent of reaction. Although the flame velocity is very slow relative to the detonation velocity, it can result in complete transformation from reactant to product in the reaction zone (order mm) if the individual hot spots are very close together (order μm). In addition, there is a mixture rule to determine the equation of state of a mixture of partially reacted material that is present in the reaction zone. The mixture rule is, for many reactive flow models, a construction

of additive volumes with pressure and temperature equilibrium enforced.[6] Other reactive flow models may use a partial pressure construction[7] or adiabatic pressure equilibrium[8-10].

Although such models are in general accord with the transformation of defects into hot spots, the coalescence of hot spots, and the subsequent detonation of the explosive, the parameter values are empirical fits to specific families of experiments. Previous model development has been focused on fitting families of experiments, using functional forms suggested by the experiments, and parameter fits to those experiments. Historically, the number of parameters has increased as each research group sought to include more and more families of experiments. This increase in complexity is not intrinsically bad, but requires each variation of explosive manufacture, age, and temperature of the experiment to be treated as a new material, subject to the same battery of experiments and parameter fitting. One outcome of our research is that we can identify some of the parameter values in the models with specific, measurable properties of the explosive. In this way, the models can be applied to a broader range of situations.

Ignition mechanisms

Field[11] describes ten mechanisms for initiation in solid explosives that are predominantly thermal localization. Most of these are associated with inhomogeneities within the explosive crystal. Some, but not all explosive crystals also show ignition from shock waves in crystals without obvious defects. PETN (pentaerythritol tetranitrate) detonates for a shock stress above 9 GPa when the shock wave is normal to the (110) or (001) planes, but the threshold exceeds 19

GPa for shocks normal to the (100) or (101) planes.[12] Other explosive crystals, such as HMX, do not detonate even when the shock pressure exceeds the explosive detonation pressure.[13] For such explosives the presence of defects is required for initiation.

Ignition by temperature localization

In explosives that are nearly theoretical density, the average temperature behind a shock front is relatively low. Table 1 shows the temperature behind a shock front for our model of HMX starting at theoretical density as a function of shock pressure. In addition, we show the time to decompose HMX to 90% final product using our three-reaction four-species model. The first two reactions are identical to those suggested by McGuire andTarver[14]. The final reaction uses the activation energy suggested by Tarver, but with the frequency factor adjusted to match the quantum molecular dynamics calculation of HMX decomposition reported by Manaa et. al.[15] The time to reaction is calculated assuming a constant pressure equal to the pressure of the incident shock. We observe that in our model, a defect-free crystal of HMX would not show transition to detonation at 40 GPa. As a consequence, defects are required to shock initiate HMX explosives at lower pressure.

Defects in explosives

High-performance explosives are assemblies of organic crystals with bimodal or trimodal size distribution. In Fig. 1, we illustrate the size distributions of HMX (1,3,5,7-tetranitro-1,3,5,7-tetraazacyclooctane) crystals for two plastic-bonded explosives (PBX). The separation of an order of magnitude or more for the peaks in the distribution and the width of the distribution are typical for all

such assemblies. Defects within the larger explosive crystals can be visualized and quantified by immersion in an index-of-refraction matching fluid and viewing with an optical microscope. The lighter color splotches in Fig. 2 are defects in the focal plane of the lens system. These HMX crystals, however, are within 0.2% of the theoretical density of the organic crystal as measured by the column gradient method. We must conclude that most of the gas-filled void of the PBX after pressing, typically 2% of the volume, is intra-granular porosity. One opportunity for this porosity is that surface irregularities may be incompletely filled by the plastic binder. These irregularities may be caused either by grinding, as are the striations on the crystal surface in Fig. 2, or steps in the crystal growth. We are at present trying to determine the gas-filled void size and morphology in PBX.

It has been recognized that if the defect and the subsequent hot spot is too small, thermal conduction to the surrounding cooler crystal will remove heat from the hot spot faster than continued decomposition can replenish it[1, 16]. As a result, there is a minimum size below which the gas-filled volume does not contribute to shock initiation. In our simulations at 1 GPa, a 1.2 μm diameter sphere of β-HMX heated to 900C decomposes and results in a steady flame propagation. Under the same conditions, a 0.8μm sphere quenches. These results are in accord with the results of Tarver et. al.[16]

Ignition near a defect

The collapse of a void is fundamentally different when the shock front is narrow relative to the void dimension, as compared to collapse by a shock front that is broad relative to the void dimension. We constructed assemblies of

explosive particles and binder at theoretical density to examine the structure of a shock after passage through such an assembly. If the stress wave is averaged over a macroscopic plane, the response is a notably longer rise time. This is caused by a statistical distribution of arrival times over the given test plane. At a specific location in that plane, the arrival time depends on the relative amount of binder and crystal that the shock has traversed. When the shock has progressed far enough down the assembly, the statistical distribution becomes steady. On the scale of the void, however, the shock is narrow. As a result, void collapse is not well described by a spherically symmetric, quasi-static compression, but by an unsymmetrical collapse from a sharp shock. Experiments and computer simulations of the collapse of simple geometric shapes (cylinders and spheres) by sharp shocks[11,17-20] have illustrated the asymmetric collapse of the void, and the localization of temperature in the gas-filled cavity and in the material surrounding the void.

Accurate simulations of this ignition process have proven difficult. Our use of Arrhenius kinetics to describe the decomposition chemistry, even with greatly simplified kinetic schemes, shows a characteristic sensitivity to temperature. The advection step taken in either ALE or Eulerian computer simulation program frameworks mixes hot gas products with cooler reactants. Parameter values and choices of sub-models for mixing that have been determined to work best for hydrodynamic simulations over the years are not necessarily the optimum choices when chemical kinetic rates must be calculated. Our results for this aspect of shock initiation must be considered preliminary.

Our first complete set of results shows the initiation of HMX around a gas-filled cavity as a function of shock pressure. The set is self-consistent, but

undoubtedly gives a result that creates too much product for a spherical hole. We also obtain the realistic result that the same cavity filled with an organic liquid (for example a solvent pocket) is much less apt to ignite. We illustrate the results in Fig. 3. There are two sources of compensating error that will tend to increase the ignition for a given shock stress when they are accounted for properly. First, defects between grains in a PBX assembly are never regular. As a result, the irregularities of the cavity will be reflected in irregularities in the temperature field that results from cavity collapse. The chemical kinetic rates will emphasize the hottest spot consistent with the dimensional requirement for sustained growth of reaction. Second, all our early simulations use a von Mises plasticity model, which collapses the spherical cavity symmetrically. In the literature, the constitutive model of the reactant is either von Mises plasticity or viscosity, which results in similarly symmetric collapse. The plasticity of these organic crystals is more complicated than von Mises plasticity. For these organic crystals, slip on a few planes is favored over most other planes. We have begun to examine the collapse of a spherical void with such a plasticity model. It is still over-simplified, but illustrates that the subsequent collapse of the cavity is not symmetric, and so leads to further temperature localization. The collapse of a cavity with a crystal plasticity model is illustrated in Fig. 4. The coupling of this plasticity model with the reaction chemistry is still in progress.

High-pressure flame propagation

In the standard view of reactive flow modeling, isolated hot spots connect with each other by deflagration to form a volume of hot products. This deflagration front moves through the unreacted solid with a velocity that

depends on pressure and temperature. We use direct numerical simulation to calculate the velocity of the deflagration. In order to simulate deflagrations at high pressure, we need complete equations of state of the various species involved, thermal transport properties of the species, and the chemical reaction kinetic rates embedded in a computer simulation program. At high pressure, species diffusion is inhibited relative to thermal diffusion.

We used the thermochemical equilibrium computer program CHEQ[21] to calculate enough points on the equation of state surface to construct a tabular equation of state in one of this laboratory's standard formats (LEOS). Historically, these thermochemical codes were unreliable estimates of states far removed from the Chapman-Jouget (CJ) adiabat. They were tuned to obtain reliable estimates of detonation properties for CHNO explosives using equation of state forms with few adjustable parameters, and with a concomitantly limited range of validity. More realistic exponential-6 molecular potentials that are now in use have led to improved estimates of the equation of state surface for a mixture of molecules with that potential.

Calculation of flame advance also requires knowledge of the transport properties. Recently, Bastea[21] has modified Enskog theory to obtain thermal conductivity consistent with the mixture of spheres represented by the exponential-6 potentials. The values he calculates at high pressure are typically within a factor of two or so of earlier estimates we made using Bridgman's model for high-density fluids. For future work in this and other related research, Bastea has also calculated consistent viscosity and species diffusivity.

To the extent that the deflagration rates are subsonic, the formulation of the numerical problem could be cast as quasistatic. However, at the small zone

size needed to resolve the deflagration front (order 10 nm), the stable time step for explicit finite-difference calculation of heat transfer is comparable to the stable time step for explicit finite-difference calculation of compressible hydrodynamics. As a result, it is numerically efficient to calculate the compressible flow dynamically. Results of those simulations at lower pressure, including assessment of the effect of various properties on the calculated deflagration speed were presented previously.[23] In summary, our calculated high-pressure deflagration speed is given by

$$v = 17 p^{0.52}$$

where the speed, v, is in m/s and the pressure, p, is in GPa. A compromise value of those parameters that are in approximate agreement with the measured deflagration speed at low pressure[24] and our calculated speed at 10 GPa is given by

$$v = 1.05 p^{1.726}$$

This functional fit for the deflagration speed is used in subsequent simulations. (Fig.5)

There is, in addition, a dependence of the deflagration speed on the temperature. We used the low-pressure dependence given by Ward et al.[25] to estimate the effect of the temperature of the reactant behind a shock front at locations away from the hot spot. It is approximately a factor of two near detonation conditions.

Growth of reaction

When the hot spots are isolated, for example a regular cubic array of hot spots, the initial behavior has precisely the same functional form as does the single void,

$$\dot{F} = 3 f_v^{1/3} \frac{v}{r_0} F^{2/3}.$$

Here F is the mass fraction of explosive consumed, f_v is the volume fraction of defects, and also the volume fraction of hot spots, which is assumed the same, and r_0 is the radius of the hot spots. When the hot spot centroids are located randomly, with no special care taken to forbid the overlap of neighbors, some hot spots will overlap from the beginning. As a result, the surface to volume ratio will increase over that of isolated spheres, so that the initial rate will be somewhat higher and the power law a will no longer be 2/3. For random arrays of hot spots, we rely on numerical simulations and fit the results to simple functional forms. We performed a family of simulations of the deflagration of clusters of hot spots varying the initial hot spot volume fraction, diameter, and the deflagration velocity. The results of those simulations can be represented by

$$\dot{F} = A f_v^{1/3} \frac{3}{r_0} v F^a (1 - F)^b,$$

where the prefactor A changes with the values of a and b. From our simulations, a is 0.63, b is 0.70 and A is 1.04.

Application of the continuum model

We used approximately 7-diameter long explosive cylinders as our computational acceptor charges, which varied between 1 and 4 mm diameter. The donor charges were all 10 mm long, and had the same diameter as the

acceptor charge, but were detonated as an ideal explosive. As a result, the acceptor charges are overdriven. We observed computationally that for those diameters in which a detonation propagated, the propagation speed decreased down the length of the charge and reached a steady value within 4 or 5 diameters of propagation. In all simulations, the radial and axial zone size was the same, 0.02 mm. Tarver and we confirmed that the results did not change when 0.01 mm zones were used. The increase in detonation speed with increasing charge diameter (Fig. 6) is in substantial agreement with the experiments performed at LANL by Campbell and Engelke.[26] The volume fraction of hot spots is taken to be the void fraction of PBX-9404, f_v=0.01, which we obtain from the ratio of the theoretical maximum density (TMD) of the explosive to the measured density. From the comparison of our simulations to the experiments, the characteristic defect has approximately 4μm diameter.

Direct simulation of hot-spots

We performed a direct numerical simulation of the passage of a 10 GPa shock in an assembly of HMX crystals (without binder) that is populated by an assembly of defects with volume fraction 2%. For this simulation of a brick 1.2mm long by 0.3mm in lateral extent, the mesh resolution is 2 μm for a total of 13.5M elements. The simulation is illustrated in Fig. 7 where the shock front has progressed about 0.3mm into the long-direction of the brick. At the end of the simulation, the shock pressure and shock velocity have transitioned to a detonation. The experimental run distance to detonation for HMX at near theoretical density is about 1 mm. In this simulation, the ignition and growth are calculated differently from the continuum model. Here the collapse of a defect

ignites a laminar flame from a point. The flame spread is described by a deflagration model. The flame is a mathematical contact surface that separates reactant from product gas within a finite-difference element. The speed of flame advance is calculated by a level-set method that can accommodate arbitrarily large numbers of ignition points, and so large numbers of individual flamelets. The flame speed is specified as a function of pressure and reactant temperature.

The calculated run distance to detonation and the thickness of the reaction zone depends on the interaction of the average spacing of the hot spots and the deflagration velocity. Errors in one of these parameters can be compensated by errors in the other.

Summary and Conclusions

Although we have traversed the path from grain-scale simulations to a continuum model, we made a number of compromises that need significantly more research to resolve. The ignition of HMX is apparently defect driven, but for other explosive crystals, direct shock initiation is apparently possible.

The ignition of energetic material by a shock wave embodies a much richer set of possibilities than we have examined. It will involve more theoretical, experimental, computational and numerical expertise than we expected at the outset. Nevertheless, the path has provided us with many insights into the orderly way in which a plastic bonded explosive proceeds from mechanical stimulus to explosion.

Acknowledgements

This research has enjoyed the enthusiastic support of Randy Simpson, the leader for explosive research in both ASC and the Munitions Technology

Development Program, during this project's formation, and throughout its life. Stew Keeton, Estella McGuire and Tom Reitter performed the numerical simulations for this project, using state-of-the-art computer hardware (that was sometimes being beta-tested by them) to do large scale computing. The ALE-3D team, under the leadership of Richard Sharp, has supported this work by modifications, improvements, and the addition of new features throughout. Of that team, we especially want to recognize several individuals. Gary Friedman created dramatic improvements in the efficiency of generating shapes, programmed the algorithms for several of the early methods of developing shapes, and served as the point of contact and interface between this project and the team; Al Nichols was responsible for the chemistry, deflagration, and heat-transfer modules in ALE-3D and frequently repaired our input files that attempted to use those modules. Rich Becker provided his model for crystal plasticity and examples as well as advice on its use. Bob Cooper, Andy Anderson, Brad Wallin, Rob Neely, and Scott Futral were also instrumental in making our progress possible.

In addition, Sorin Bastea provided equations of state with CHEQ, and also developed methods to calculate consistent transport properties for the explosive products. Riad Manaa's Quantum Molecular Dynamics simulations of the decomposition of HMX at high temperature and pressure have given us a benchmark for testing our simplified chemical kinetics reaction scheme at high pressure and temperature. Craig Tarver provided his unpublished parameters for reactive flow modeling of PBX-9404 in small diameter charges, and freely shared his expertise in applying reactive flow models to calculations of macro-scale phenomena. Ed Lee provided a willing ear and the voice of reason for most

of our nascent ideas. A number of extended discussions with Ralph Menikoff, LANL, have provided us with an alternative point of view on cavity collapse. His thoughtful comments have been very helpful to us in analyzing our results.

This work was performed under the auspices of the U.S. Department of Energy by University of California, Lawrence Livermore National Laboratory under Contract W-7405-Eng-48.

References

1. Bowden, F.P. and Yoffe, Y. D. Initiation and Growth of Explosion in Liquids and Solids, Cambridge University Press, New York, 1952 (Reissued in the Cambridge Science Classics series, 1985)

2. Campbell, A. W., Davis, W. C., Ramsay, J. B. and Travis, J. R., 1961, Phys. Fluids 4, 511.

3. Mader, C.L., 1963, Phys. Fluids, 6, 1811.

4. Field, J.E., Swallowe, G. M., Heavens, S.N., 1982, Proc. R. Soc. London, A382, 231.

5. Bourne, N.K. and Field, J.E., 1999, Proc. R. Soc. London, A455, 2411.

6. Lee, E.L. and Tarver, C.M., 1980, Phys. Fluids, 23, 2362.

7. Souers, P.C., Garza, R. and Vitello, P., 2002, Prop. Expl. Pyrotech., 27, 62.

8. Cowperthwaite, M., 1981, 7th Symposium (International) on Detonation, Annapolis, MD, 498.

9. Partom, Y., 1981, 7th Symposium (International) on Detonation, Annapolis, MD, 506.

10. Reaugh, J.E. and Lee, E.L., 2002, 12th Symposium (International) on Detonation, San Diego, CA (in press).

11. Field, J.E., 1992, Acc. Chem. Res., 25, 489.

12. Dick, J.J., Mulford, R.N., Spencer, W.J., Pettit, D.R., Garcia, E. and Shaw, D.C., 1991, J. Appl. Phys., 70, 3572.

13. Campbell, A.W. and Travis, J.R., 1985, 8th Symposium (International) on Detonation, White Oak, Md, 1057.

14. McGuire, R.R. and Tarver, C.M., 1981, Proceedings, 7th Symposium (International) on Detonation, Annapolis MD.

15. Manaa, M.R., Fried, L.E., Melius, C.F., Elstner, M. and Frauenheim, T.H., 2002, J. Phys. Chem. A, 106, 9024.

16. Tarver, C.M., Chidester, S.K., and Nichols, A.L., 1996, J. Phys. Chem., 100, 5794.

17. Mader, C.L., 1979, Numerical Modeling of Detonations, University of California Press, Berkeley, CA,171

18. Bourne, N.K. and Milne, A.M., 2002, 12th Symposium (International) on Detonation, San Diego, CA (in press).

19. Bourne, N.K. and Milne, A.M., 2003, Proc. R. Soc. Lond. A459, 1851.

20. Menikoff, R., 2003, Shock Waves in Condensed Matter, Portland, OR (in press).

21. Ree, F.H., 1984, J. Chem. Phys., 81, 1251.

22. Bastea, S., 2002, 12th Symposium (International) on Detonation, San Diego, CA (in press).

23. Reaugh, J.E., 2003, Shock Waves in Condensed Matter, Portland, OR (in press).

24. Boggs, T.L., 1984, Progress in Astronautics and Aeronautics, AIAA, NY,121.

25. Ward, M.J., Son, S.F. and Brewster, M.Q., 1998, Combustion and Flame, 111, 556.

26. Campbell, A.W. and Engelke, R., 1976, 6th Symposium (International) on Detonation, White Oak, MD, 642.

Figure captions

Figure 1. Particle size distribution of HMX for LX04 (solid) and PBX9501 (dash) plastic bonded explosives.
Figure 2. Photomicrographs of HMX illustrating the crystal defects 2a and defects on the crystal surface 2b. The largest particles in the photo are approximately 100 μm.
Figure 3. Calculated formation of HMX decomposition product as a function of time for shocks of various strengths. The fluid-filled cavity threshold is larger than 10 GPa.
Figure 4. Collapse of a void using crystal plasticity model. The fringe colors indicate the total slip. The maximum equivalent plastic strain is 300%.
Figure 5. Calculated deflagration speed as a function of pressure including compromise fit
Figure 6. Results of the continuum model for three different defect sizes. All other parameters were determined by results of grain-scale simulations.
Figure 7. Propagation of a 10 GPa shock wave in a block of HMX 1.2mm x 0.3mm x 0.3mm with 2% void volume. Spheres in front of the shock front are the defects. The flame fronts arising from each shock-collapsed defect behind the shock front begin to coalesce.

Tables

Table 1. Temperature behind a shock in defect-free HMX, and the time required for the complete decomposition of HMX at that initial temperature and constant pressure.

Shock pressure, GPa	Shock temperature, K	Time, sec
10	633	1.06×10^{6}
15	894	1.32×10^{5}
20	1196	2.64×10^{4}
25	1523	5.21×10^{3}
30	1885	6.17×10^{2}
35	2258	2.33×10^{1}
40	2653	2.55×10^{-2}

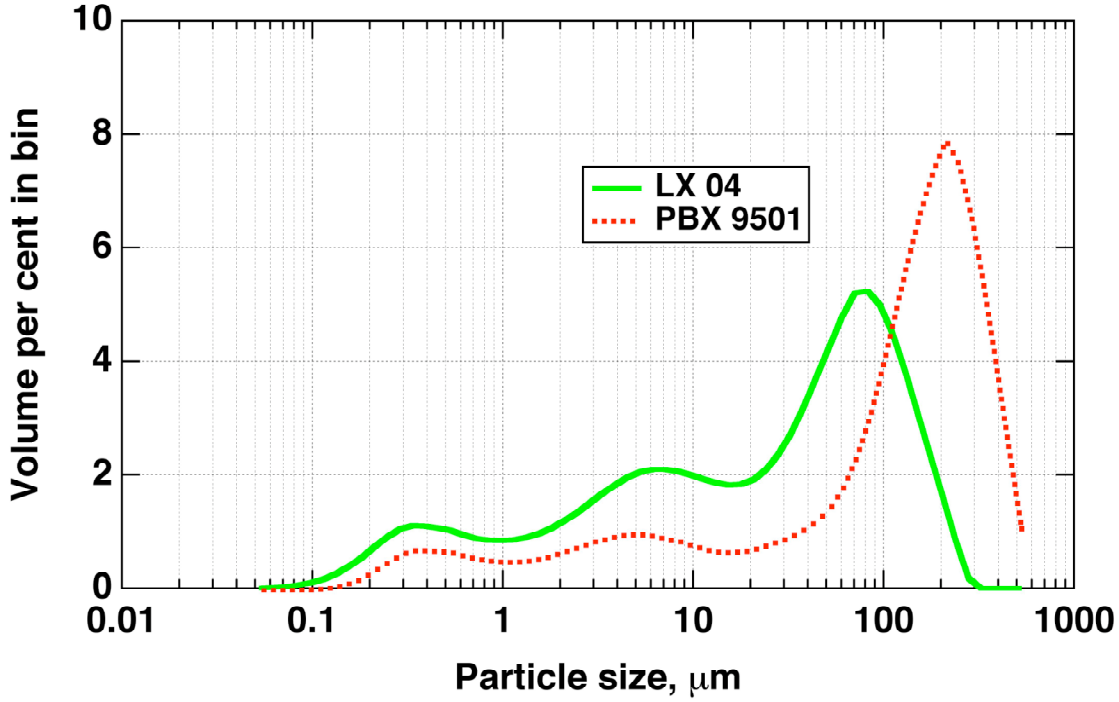
Volume per cent in bin
Particle size, μm
LX 04
PBX 9501
0
2
4
6
8
10
0.01
0.1
1
10
100
1000

Figure 1.

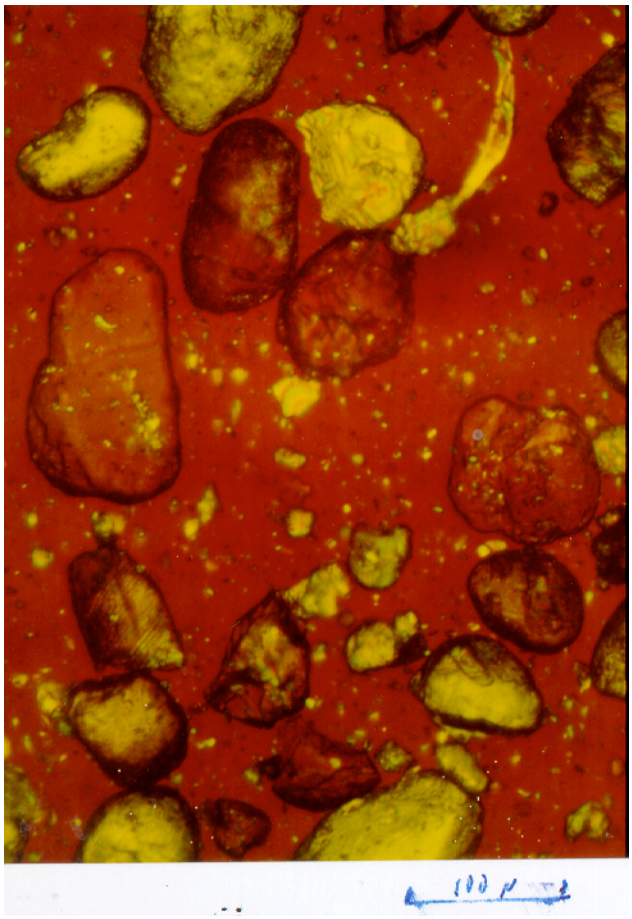

Figure 2a

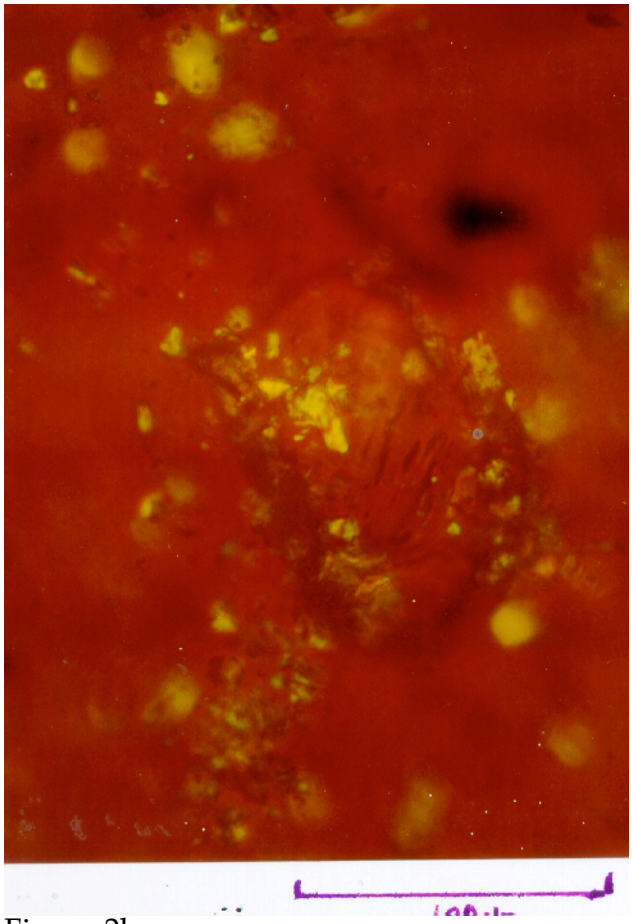

Figure 2b

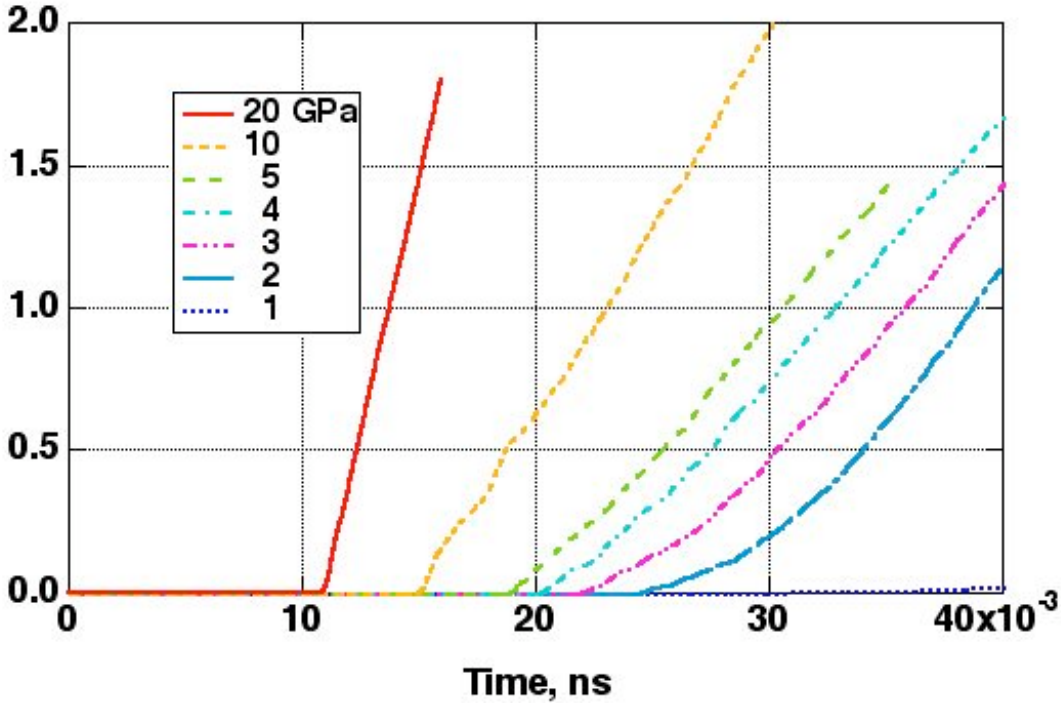

Figure 3.

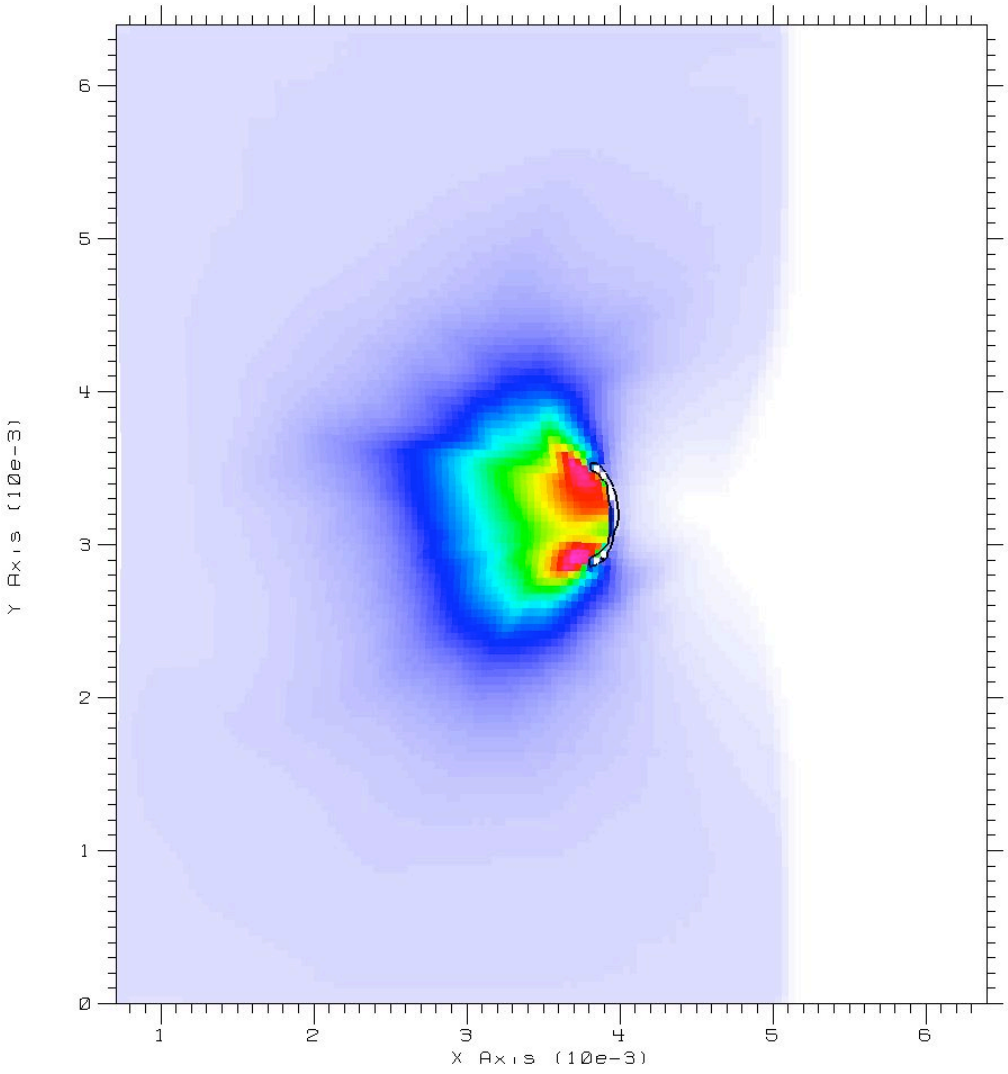

Figure 4.

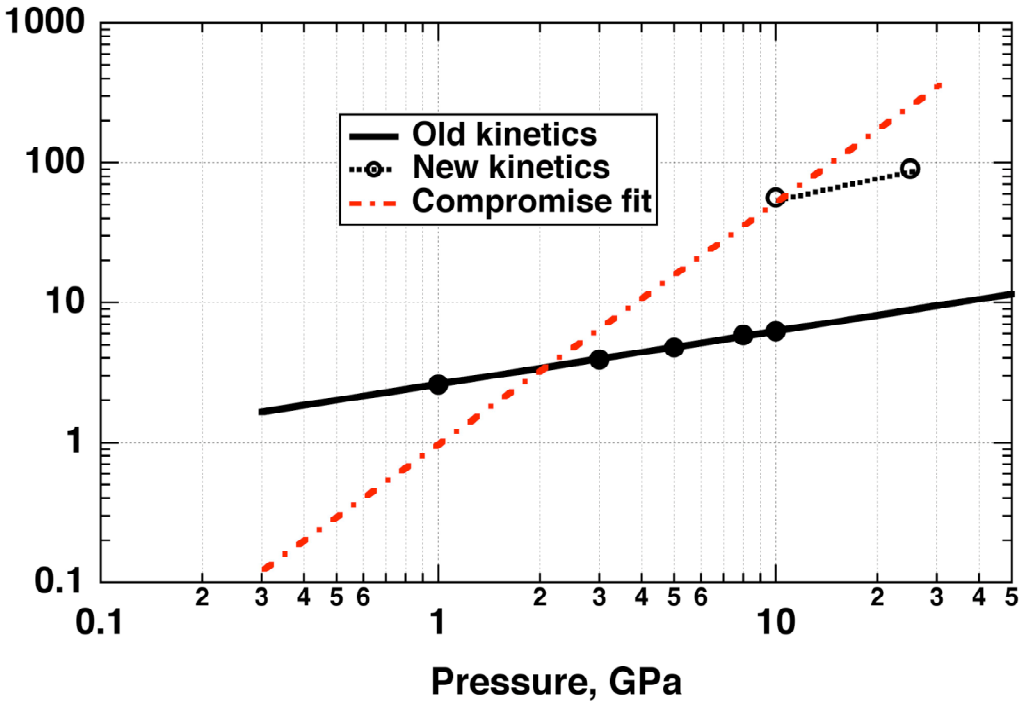
1000
100
10
1
0.1
Old kinetics
New kinetics
Compromise fit
0.1
1
10
Pressure, GPa

Figure 5.

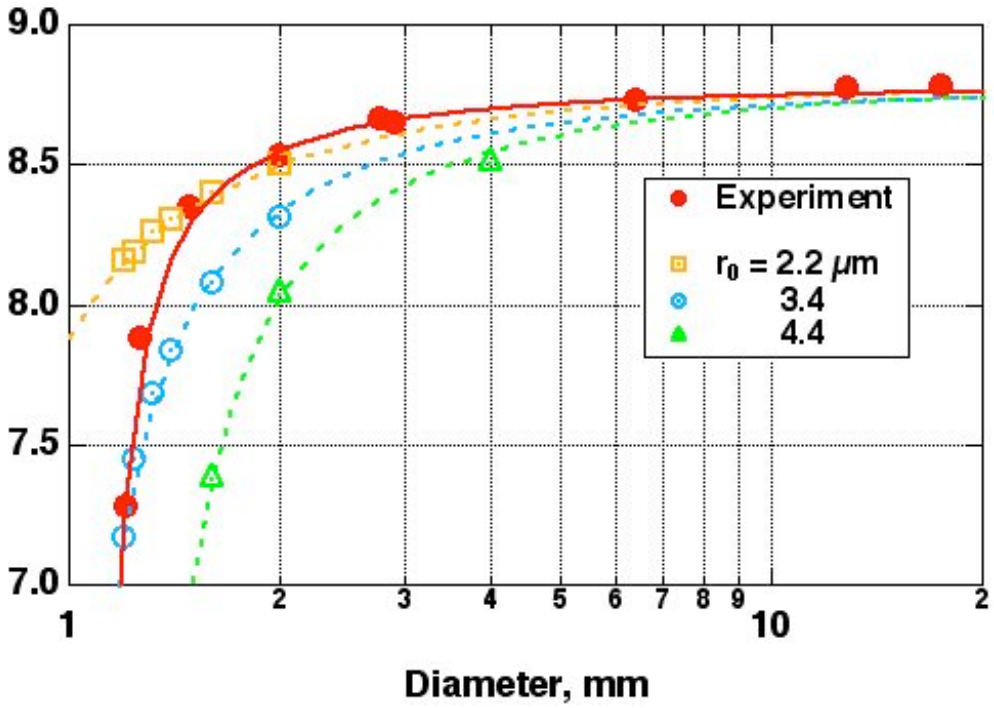
9.0
8.5
8.0
7.5
7.0
1
2
3
4
5
6
7
8
9
10
2
Diameter, mm
Experiment
r0 = 2.2 μm
3.4
4.4

Figure 6.

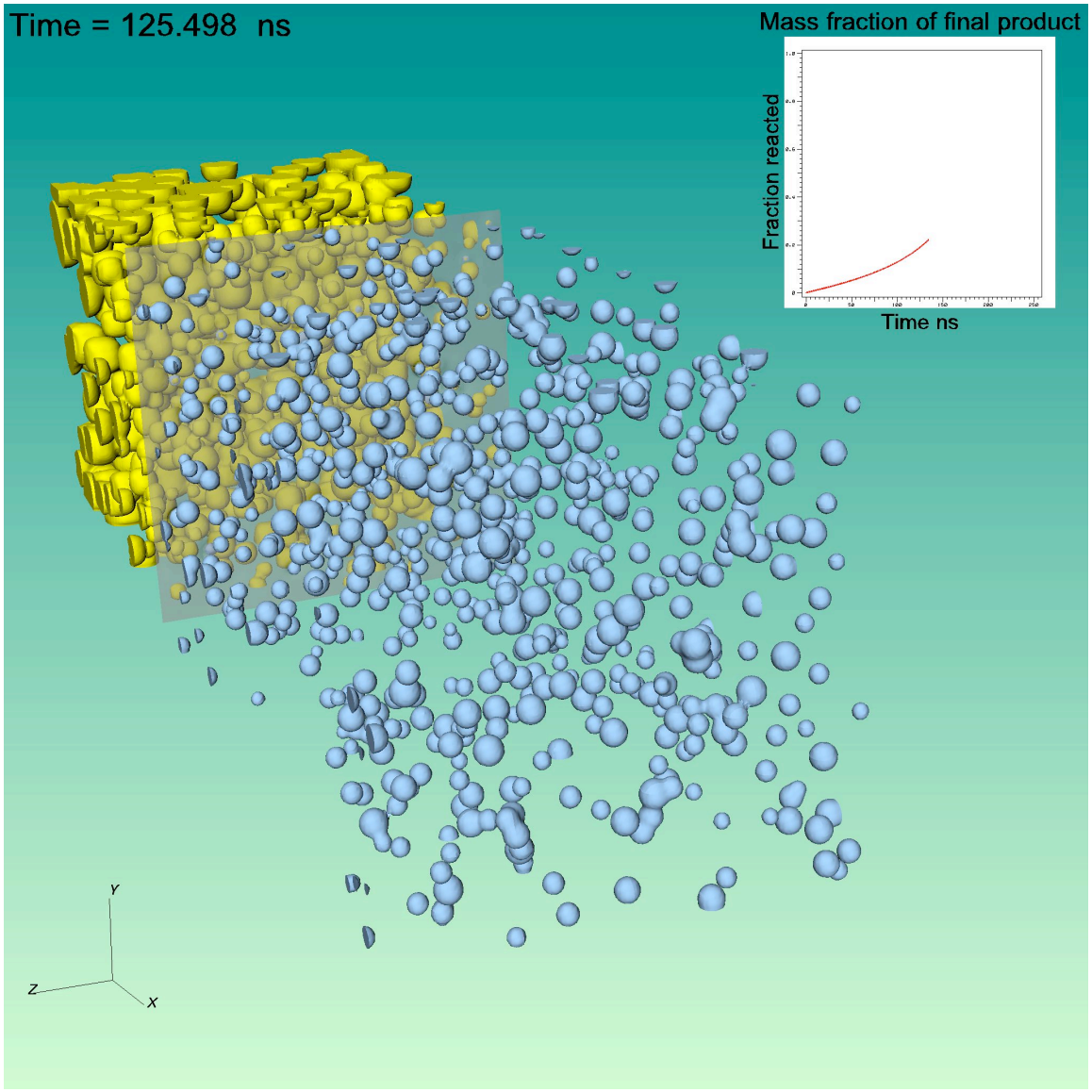
Time = 125.498 ns
Mass fraction of final product
Fraction reacted
Time ns
Y
Z
X

Figure 7.

University of California
Lawrence Livermore National Laboratory
Technical Information Department
Livermore, CA 94551